11-15-2017

A Comparison of Sensitivity Metrics for Two-Stage Ignition Behavior in Rapid Compression Machines

David Wilson
Marquette University

Casey Allen
Marquette University, casey.allen@marquette.edu

Accepted version. *Fuel*, Vol. 208 (November 15, 2017): 305-313. DOI.

A comparison of sensitivity metrics for two-stage ignition behavior in rapid compression machines

David Wilson
Department of Mechanical Engineering, Marquette University, Milwaukee, WI
Casey Allen
Department of Mechanical Engineering, Marquette University, Milwaukee, WI

Abstract

A rapid compression machine (RCM) multi-zone model is used to simulate the ignition of primary reference fuel (PRF) mixtures that exhibit two-stage ignition behavior. Sensitivity coefficients for each reaction in the PRF mechanism are calculated from four different metrics: (1) first-stage energy release, (2) first-stage pressure rise, (3) first-stage ignition delay time, and (4) total ignition delay time. The sensitivity coefficients are used to provide four unique rankings, and the rankings are compared using Spearman's rank correlation coefficient. Special emphasis is given to comparing the rankings based on first-stage energy release and total ignition delay time. The level of agreement between these two rankings is shown to depend on the reaction conditions. Simulation cases with high peak heat release rates during the first stage of ignition tend to exhibit disagreement in the rankings, indicating that new kinetic information can be obtained by studying first stage energy release in addition to total ignition delay time. Simulations show that the high peak heat release rates are associated with energy release across a broad range of temperatures (range can be in excess of 100 K even for lean conditions). This distribution leads to a discrepancy between sensitivity coefficients

calculated for the total ignition delay time and the first-stage energy release. Sensitivity coefficients for the total ignition delay time are characterized by reactivity at the highest temperatures in the RCM, while sensitivity coefficients for the first-stage energy release are characterized by reactivity across the full range of temperatures in the RCM.

Keywords
Rapid compression machine, Ignition delay time, Two stage ignition, Sensitivity analysis

1. Introduction
Accurate kinetic models are an integral part of the workflow for improving combustion technology. By including these models within a larger reacting flow simulation, local rates of species formation and destruction and the corresponding energy release rates can be predicted. There is a widespread effort to validate and improve these models by conducting fundamental experiments under well-characterized conditions. Data from these experiments are compared with simulation predictions to assess the accuracy of a kinetic model, and when disagreement between the data and model exists, sensitivity analysis is frequently used to discern which reaction or set of reactions should be prioritized for improvement.

Rapid compression machine (RCM) experiments are one type of fundamental test used to validate kinetic mechanisms. The tests consist of measuring pressure during the ignition of a fuel-oxidizer mixture. The overall shape of the curve reflects the combined effects of chemical heat release, heat loss, crevice flow, and ringpack blowby. A model-based approach may be used to interpret these data to define an instantaneous heat release rate, but currently no such model implementation exists. Rather, the data are traditionally used to define one or more ignition delay times depending on whether the fuel exhibits single or two-stage ignition. These global metrics are used as the basis for conducting sensitivity analysis in RCM simulations.

The end use of kinetic models within engine computational fluid dynamics (CFD) codes requires they make accurate reaction rate predictions for widely varying in-cylinder conditions. It is important to consider that ignition delay data used to optimize kinetic mechanisms may not be sensitive to all the chemical pathways that are relevant to energy release within the engine cylinder, which is especially relevant for modeling apparent heat release rates calculated from engine data. This paper considers the definition of two additional metrics that can be used with RCM experiments to investigate the roles of these reactions for two-stage ignition fuels. These metrics are the total first stage energy release (ΔH_1) and the total pressure rise during the first stage of ignition (ΔP_1) The authors hypothesize that these metrics will be sensitive to the full distribution of temperatures within the RCM, and therefore sensitive to a set of reactions that may be unique from the controlling chemistry for the first stage and total ignition delay times. ΔH_1 is proposed for study because it is a proxy to directly validating heat release rate in the RCM, and ΔP_1 is proposed because it can be easily calculated from pressure data obtained during a RCM experiment. Although ΔH_1 can be calculated from RCM data, its accuracy is highly dependent on the rigor of the model used to interpret the pressure data. To determine the value of ΔH_1 and ΔP_1 as validation metrics, this paper presents sensitivity analysis with respect to the four metrics of ΔH_1, ΔP_1, τ (total ignition delay time) and τ_1 (first stage ignition delay time). The results are analyzed to identify the important chemical reactions for governing these phenomena.

For fuels/tests that exhibit two-stage ignition, RCM experiments show that the hot ignition timing is influenced by the energy released during the first stage of ignition. Experiments reported by Tanaka et

al. [1] showed that as the pressure rise due to first stage ignition increased, the total ignition delay time decreased. Tanaka et al. indicate this occurs because increases in pressure rise due to first stage activity correspond to higher gas temperatures that accelerate the onset of hot ignition. This is consistent with the interpretation of Ribaucour et al. [2] and later reaffirmed by Westbrook [3], that the onset of hot ignition is controlled by a critical temperature at which H_2O_2 decomposes rapidly. The time at which a mixture reaches this condition in a RCM experiment was shown to depend on the timing and magnitude of energy release in the first stage of ignition. Additional studies in the literature demonstrate the dependence of first stage energy release on the reaction conditions. The simulations of Zhao and Law [5] quantified the influence of equivalence ratio and reaction temperature (*i.e.*, the "compressed temperature" in RCM experiments) on the first stage temperature rise and therefore the total ignition delay time. Zhang et al. [4] quantified the role of unique factors influencing negative temperature coefficient behavior (NTC), showing that the temperature rise due to first stage energy release plays a substantial role in determining the total ignition delay time. Given the evidence from these prior works, reactions that strongly influence τ_1 and ΔH_1 (or ΔP_1) should also strongly influence τ. There is limited data in the literature to support this view, however, because the majority of sensitivity analyses use a sensitivity metric based on τ alone, with τ_1 being neglected. Some exceptions to this include the dimethyl ether study (DME) by Mittal et al. [6] and the gasoline surrogate works of Kukkadapu et al. [7], [8]. In their study of DME ignition behavior, Mittal et al. reported that the most influential reaction for both τ_1 and τ was the isomerization of the methoxymethyl-peroxy radical [6]. However, inspection of their results suggests a difference in ranking for other reactions. Kukkadapu et al. [5] calculated sensitivity coefficients for τ_1 and τ in the low-temperature, lean-to-stoichiometric region using an adiabatic, constant volume simulation. The analysis was based on a brute force method and considered a four-component surrogate of iso-octane, *n*-heptane, toluene, and 2-pentene. The largest sensitivity coefficients for τ_1 were associated with H-atom abstraction reactions by OH from parent fuel molecules (namely *n*-heptane and iso-octane) and isomerization reactions of heptylhydroperoxy radicals. These same reaction classes were also influential for the total ignition delay time, further supporting the dependence of τ on τ_1. A relationship between τ and τ_1 is clearly supported by these studies, but the relationship is not well characterized as it is often based on analysis at only one or a few conditions.

The main objective of this paper is to compare and contrast the governing chemistries for the RCM validation metrics of ΔH_1, ΔP_1, τ and τ_1 for a variety of test conditions. The basic approach used is to conduct brute force sensitivity analysis on the metrics for a wide range of RCM simulation cases. By understanding these metrics and their sensitivities, RCM experiments may be optimally designed to probe a reaction or reaction set of interest. This will enable more comprehensive analysis of RCM data that can be used to improve kinetic models.

2. Methods

2.1. Modeling approach

To rigorously characterize the reaction sensitivities at a given test condition, all of the important reactor physics must be modeled. This is accomplished in this work by use of a multi-zone model (MZM) designed to simulate the heat loss, crevice flow, and chemical energy release during an RCM experiment [9], [10]. The model divides the main reaction chamber into a set of concentric zones, each with a characteristic temperature and composition that evolves during the simulation. The zones communicate with one another by conduction only, as there is no mass transfer between the zones.

The influence of the crevice and ringpack flows on the main chamber conditions are also modeled, assuming quasi-steady flow through the tapered gap that connects the crevice to the main chamber. The model is implemented in Python Cantera, and has been validated to yield cylinder-averaged speciation predictions within 15% of those predicted by computational fluid dynamics (CFD) [9]. All simulations were conduced with 15 zones in the main reaction chamber, and the simulations were terminated upon reaching an average cylinder temperature of 1200 K. The RCM modeled in this paper has an 8 inch stroke and a 2 inch bore. A single arbitrary velocity profile was used for all of the simulations, with a compression time of 32 ms. Depending on the compression ratio for a given simulation case, the modeled RCM piston has a crevice volume between 9% and 13% of the reaction chamber volume at top dead center (TDC). Use of the MZM for this study is very important because reliable predictions of the RCM sensitivity metrics ΔH_1, ΔP_1, and τ cannot be obtained during multi-stage ignition events using constant volume or effective volume modeling techniques [11]. The ΔH_1 and ΔP_1 metrics are particularly sensitive to the temperature distribution in the RCM, thus single zone models are inadequate for conducting the sensitivity analysis presented in this work. In fact, modeling the RCM reactor physics is critical to this work because they strongly influence our observations of ignition behavior. It is noted that ΔH_1 is used in this study as a metric because it serves as a proxy to the temperature increase during first stage ignition. Section 1 describes how the temperature increase due to first stage ignition is important for determining the hot ignition timing, and this increase is driven by ΔH_1.

The PRF mechanism of Tsurushima [12] is used in this work primarily because it is compact (33 species and 38 reactions), and because it is capable of modeling two-stage ignition behavior. The model was developed using the PRF mechanism of Tanaka et al. [13] as a baseline, and it has been validated with shock tube ignition delay data in the temperature range of 700–1200 K and the pressure range of 6–42 bar. However, given that the objective is to characterize reaction sensitivities with respect to ignition phenomenology, the predictive accuracy of the mechanism is of reduced importance. It would be preferable to conduct this investigation with a detailed mechanism, but this would be impractical due to the computational burden of simulating fuels that exhibit two-stage ignition.

2.2. Analysis procedure for simulation results

The MZM is used in this work to simulate all of the test cases described in the following section. Sample simulation output for one of the tests appears in Fig. 1 so that the metrics used to characterize the simulations can be described. Fig. 1(a) shows the reaction chamber pressure predictions for the simulation with the metrics of τ_1 and τ illustrated. τ_1 is defined as the interval between the end of compression (i.e., top dead center, at t = 0.0 s) and time of peak heat release rate, which is shown in Fig. 1(c). This time is also coincident with the peak in the pressure derivative with respect to time (dP/dt), shown in Fig. 1(b). The total ignition delay time, τ , is defined as the interval between TDC and

the main ignition event, which was assumed to have occurred once the average cylinder temperature reached 1200 K. All simulations were terminated after reaching this condition.

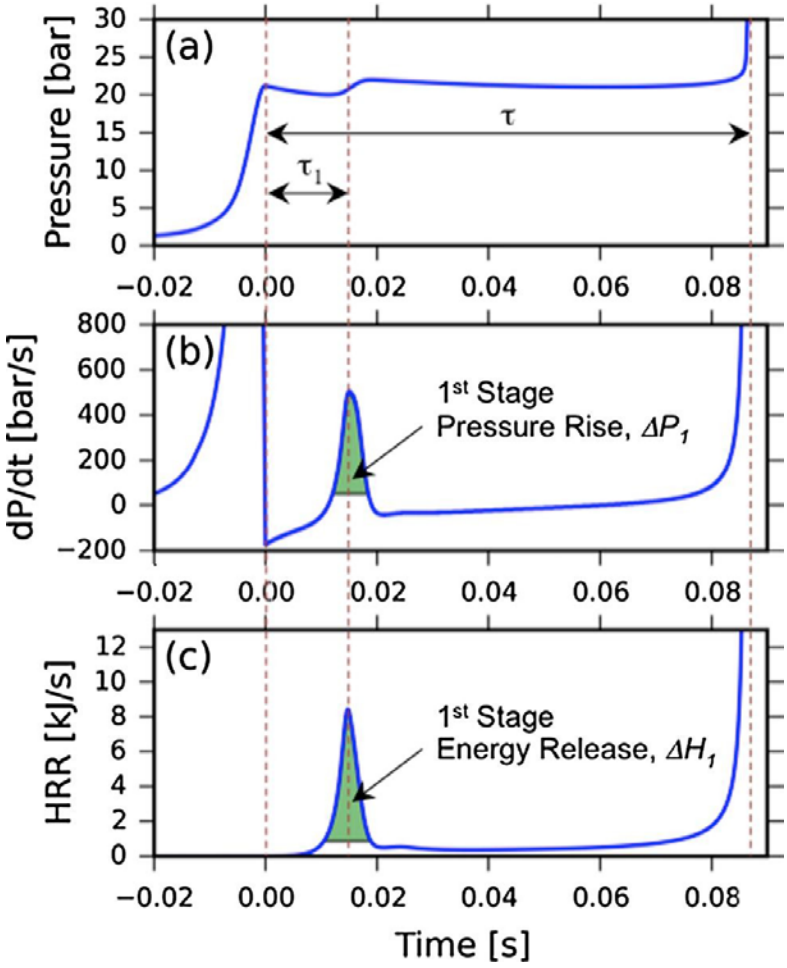

Fig. 1. Illustration of metrics used to characterize the simulation results, including (a) reaction chamber pressure, (b) reaction chamber pressure derivative with respect to time (dP/dt), and (c) total cylinder rate heat release rate (HRR). All predictions are from the same simulation, with the initial conditions T_0 = 306 K, P_0 = 1.08 bar, ϕ = 0.47, Fuel: PRF 68, and r_c = 9.8.

Fig. 1(b) also illustrates the ΔP_1 metric, which represents the pressure rise due to first stage energy release. ΔP_1 is calculated by integrating the area under the dP/dt curve where dP/dt is greater than or equal to 10% of the maximum dP/dt observed during the first stage of ignition. These integration bounds are represented by the shaded region under the dP/dt curve in Fig. 1(b). A similar approach is used to calculate the ΔH_1 metric, as illustrated in Fig. 1(c). Here, ΔH_1 is calculated by integrating the HRR data in the domain where the HRR is greater than or equal to 10% of the maximum HRR observed during the first stage of ignition.

Given the apparent importance of first stage energy release for the overall reaction trajectory, sensitivity analysis is conducted here to determine whether the important reactions for first stage energy release are the same as the important reactions for the first stage and/or total ignition delay times. A brute-force sensitivity analysis approach is used to examine the percent sensitivity for the following metrics: τ_1, τ, and ΔH_1, and ΔP_1. In this approach, a baseline simulation is conducted with the pre-exponential factors for all reactions at their nominal values. Following this, one additional simulation is conducted for each reaction in the mechanism, allowing the corresponding pre-

exponential factors to be doubled one-at-a-time. The results of the simulation set are used to calculate sensitivity coefficients as

(1)

$$S_{\Gamma,i} = 100\% \cdot \frac{\Gamma(2k_i) - \Gamma(k_i)}{\Gamma(k_i)}$$

Where Γ corresponds to any of the given combustion metrics (*i.e.*, τ) and i represents the reaction number. In this manner, the following sensitivity coefficients are calculated for each reaction: $S_{\tau,i}$, $S_{\tau_1,i}$, $S_{\Delta H_1,i}$, and $S_{\Delta P_1,i}$. The sensitivity coefficients are used to rank the importance of the reactions.

2.3. Test cases

A total of 280 unique test conditions were simulated using the MZM. To facilitate the sensitivity analysis described previously, a total of 39 simulations were conducted for each of the unique test conditions. This yielded a total of 10,920 MZM simulations with a corresponding wall time of approximately 50 days.

The initial conditions for the simulations were randomly sampled from a parameter space for initial temperature (T0), compression ratio (rc), iso-octane (i-C8H18) fuel volume percentage (i.e., octane number or ON) and equivalence ratio (φ). All simulations were conducted with an initial pressure of P0 = 1.08 bar. It is possible that a sampled point may not be viable for the sensitivity analysis described here because of heat release during the compression stroke or a failure to ignite within a reasonable time (<200 ms after TDC). To avoid executing a series of costly MZM runs under these conditions, all sampled points are quickly screened with a constant volume, adiabatic bomb simulation. The simulations are initialized with a temperature and pressure that is estimated by assuming isentropic compression of an ideal gas from the initial conditions that have been sampled. These isentropic calculations utilize a heat capacity ratio of γ = 1.34, which was selected from preliminary analysis using the MZM. This “effective” heat capacity ratio yielded approximate agreement (typically less than 10 K) between the isentropic calculation and the maximum temperature obtained from a MZM simulation. Sampled test points were accepted for use in the MZM simulations if the corresponding bomb simulation produced a total ignition delay time between 10 and 150 ms and a heat release rate not exceeding 5 kJ/s prior to t = 10 ms in the simulation. These criteria resulted in a set of simulation conditions that spanned the lower and upper limits described in Table 1. The conditions at TDC are characterized by the compressed temperature (Tc) and compressed pressure (Pc) that appear in the table. The test conditions correspond to the low-temperature, lean combustion conditions that are important for advanced compression ignition engines.

Table 1. Simulated test conditions.

Number of Simulation Conditions: 280		
	Lower Limit	**Upper Limit**
T_0	300 K	339 K
r_c	7.0	10.2
T_c	620 K	685 K
P_c	13.9 bar	22.6 bar
ON (vol-% iC_8H_{18})	1.1	70.6
ϕ	0.28	0.50
τ_1	6.5 ms	90.4 ms

τ	18.5 ms	150.4 ms

2.4. Statistical analysis

The sensitivity coefficients that are calculated for the metrics of τ_1, τ, ΔH_1, and ΔP_1 are used to independently rank the importance of the reactions, resulting in four unique rankings. The rankings for these metrics are compared in two different ways. First, a comparison is made between the three most important reactions for each of the metrics because three represents a reasonable upper limit for the number of reactions that may be targeted for improvement within a given project. Often times, only one or two reactions are considered for improvement once being identified as the important reactions for governing some global phenomena. Ranking of the reactions beyond this point might be considered irrelevant because the ranking is not used. However, to get an overall comparison of the reaction rankings, a second comparison is made using Spearman's rank correlation coefficient [14]. Spearman's rank correlation coefficient is chosen for this purpose because the rankings exhibit monotonic relationships, but are not always linear, which would be required to utilize Pearson's product-moment correlation. Spearman's rank correlation coefficient ($\rho_{j,k}$) is calculated as

(2)

$$\rho_{j,k} = 1 - \frac{6\sum d_i^2}{n(n^2-1)}$$

where *j* and *k* correspond to the two independent variables used to rank the data. *n* is the number of reactions being ranked (*n* = 38) and d_i is the difference between the rank values of reaction *i* given by two different metrics. For example, presume that reaction 12 has the 3rd largest S_{τ_1} value and the 8th largest $S_{\Delta H_1}$ value. Then $d_{12} = 8 - 3 = 5$ for $\rho_{\Delta H_1,\tau_1}$. Note that if the rankings by two metrics were the same, then $d_i = 0$ for all reactions and $\rho_{j,k} = 1$ for the two metrics. Deviation from $\rho_{j,k} = 1$ indicates non-monotonicity between the rankings. The following rank correlation coefficients are calculated in this work for each of the simulation cases summarized in Table 1: $\rho_{\Delta H_1,\tau_1}$, $\rho_{\Delta H_1,\tau_1}$, and ρ_{τ,τ_1}.

3. Results and discussion

3.1. Overall comparison of rankings

A summary of the rank correlation coefficients is shown in the histogram in Fig. 2. The histogram considers the full set of simulation conditions described in Table 1, and the results show that the lower and upper limits of the rank correlation coefficients are:

$$0.40 \leqslant \rho_{\tau_1,\tau} \leqslant 0.80,$$

$$0.31 \leqslant \rho_{\Delta H_1,\tau_1} \leqslant 0.81, \text{ and}$$

$$0.67 \leqslant \rho_{\Delta H_1,\tau} \leqslant 0.97.$$

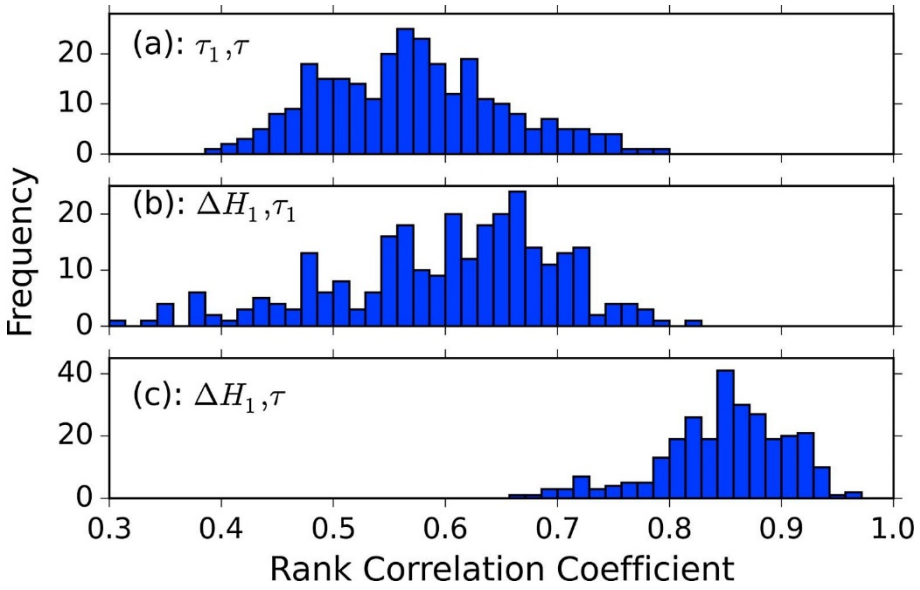

Fig. 2. Histograms of Spearman's rank correlation coefficient for (a) $\rho_{\tau_1,\tau}$, (b) $\rho_{\Delta H_1,\tau_1}$, (c) $\rho_{\Delta H_1,\tau}$.

The mean values for the rank correlation coefficients are $\rho_{\tau_1,\tau} = 0.57$, $\rho_{\Delta H_1,\tau_1} = 0.60$, and $\rho_{\Delta H_1,\tau} = 0.85$. These results point toward discrepancies in the rankings of reaction importance based on these different metrics. Regarding the distributions, it is noteworthy to consider the broad upper and lower limits observed for the rank correlation coefficients. This points to substantial variation in the agreement between the rankings, and the level of agreement appears to be sensitive to the reaction conditions being simulated. Analysis is presented in Sections 3.4 Influence of reaction conditions on rank agreement, 3.5 Influence of reaction behavior on rank agreement to support this view, and to understand how the test conditions and reaction phenomenology influence the magnitude of the rank correlation coefficients.

The authors note that the low values for ρ_{τ,τ_1} may suggest the controlling chemistry differs between the first stage energy release and the main ignition event. However, references to "controlling chemistry" should really be based on a comparison of the most influential reactions, not a ranking of the full set. Disagreement in rank sequence between low priority reactions could also lead to small rank correlation coefficients, but such disagreement would be irrelevant in the prioritization of reactions for further study. A comparison between the rankings for the most influential reactions appears in Section 3.3.

Fig. 2(b) and (c) shows that the reaction rankings based on ΔH_1 exhibit greater similarity to the rankings given by τ than by τ_1. This result is consistent with the phenomenological understanding that the amount of energy released during the first stage of ignition influences the onset of the main ignition event. Given this better agreement between the $S_{\Delta H_1}$ -based and S_τ -based rankings, the authors have chosen to focus the additional analysis in Sections 3.4 Influence of reaction conditions on rank agreement, 3.5 Influence of reaction behavior on rank agreement on characterizing the relationship between these sets of rankings and how it is influenced by the reaction conditions. The relatively low values of $\rho_{\Delta H_1,\tau_1}$ indicate substantial differences between the $S_{\Delta H_1}$ -based and S_{τ_1} -based rankings, meaning the ΔH_1 metric offers new kinetic information not available through study of τ_1. However, that kinetic information may be redundant to information obtained through study of τ in cases where $\rho_{\Delta H_1,\tau}$ is large. Hence, our interest is to identify the conditions where $\rho_{\Delta H_1,\tau}$ is large.

Hence, our interest is to identify the conditions where $\rho_{\Delta H_1,\tau}$ is small, suggesting that unique kinetic insight can be had by studying ΔH_1.

3.2. Illustration, significance, and trends of the rankings

To illustrate the significance of the $\rho_{j,k}$ magnitudes, Fig. 3 compares the reaction rankings based on ΔH_1 and τ for three different $\rho_{\Delta H_1,\tau}$ values (0.71, 0.84, 0.97). The values were chosen to illustrate poor, moderate, and good agreement between the rankings. The plots in Fig. 3(a), (b), and (c) show the full ranking comparison, and the same data is shown in plots Fig. 3(d), (e), and (f), respectively, but with a reduced scale. By comparing Fig. 3(a)–(c), it is seen that a rank correlation coefficient change between limits of 0.71 and 0.97 corresponds to a significant difference in reaction ranking agreement. For points that exist on or near the red dashed line, the reaction rankings obtained with the two metrics are similar, which is the case for many of the reactions in the $\rho_{\Delta H_1,\tau} = 0.97$ case (Fig. 3(c)). In Fig. 3(a), however, many of the points deviate substantially from the line, indicating that the important reactions for governing ΔH_1 and τ are different. Much of this deviation occurs in the high-rank region (i.e., reaction rank ≤ 10), meaning it would be influential for investigators prioritizing a small subset of reaction rate constants for improvement. The plots in Fig. 3(d), (e), and (f) have been scaled to show only the "high-rank region", and the significance of the gray dashed lines is described in Fig. 3(d). These lines are drawn at the lowest reaction rank that has a sensitivity coefficient of at least 40% of the sensitivity coefficient of the most important reaction. For example, in Fig. 3(d), the horizontal gray dashed line is drawn at *Reaction Rank* by $\tau = 6$, meaning that $S_{\tau,i} \geqslant 0.4 \cdot S_{\tau,1}$ for all reaction ranks i ≤ 6 (i.e., the six most important reactions). The 40% cutoff has been chosen arbitrarily to visually identify which reactions are significant within the ranking sequence. When the same criterion/threshold is applied to the $S_{\Delta H_1}$ -based rankings, a vertical gray dashed line is drawn at *Reaction Rank by* $\Delta H_1 = 1$. This indicates that $S_{\Delta H_1,1}$ is at least 2.5 times greater (*i.e.*, 1/0.4) than any of the other sensitivity coefficients. These cutoff lines are used to identify four regions: (A), (B), (C), and (D). Reactions that are ranked within region (A) are identified as important by both $S_{\Delta H_1}$ -based and S_τ -based rankings. By contrast, reactions that are ranked within region (D) do not exert significant influence over either the ΔH_1 or τ metrics. The existence of rankings in either regions (B) or (C) point toward the complementary nature of the $S_{\Delta H_1}$ -based and S_τ -based rankings. Region (B) contains reactions that are important for τ, but not for ΔH_1 while region (C) contains reactions that are important for ΔH_1, but not for τ. As one specific example, it is interesting to note that for the $\rho_{\Delta H_1,\tau} = 0.84$ case, the second most important reaction based on $S_{\Delta H_1}$ is the 25th most important reaction according to S_τ (Fig. 3(b)). This type of disagreement suggests that complementary kinetic information can be obtained by studying both ΔH_1 and τ.

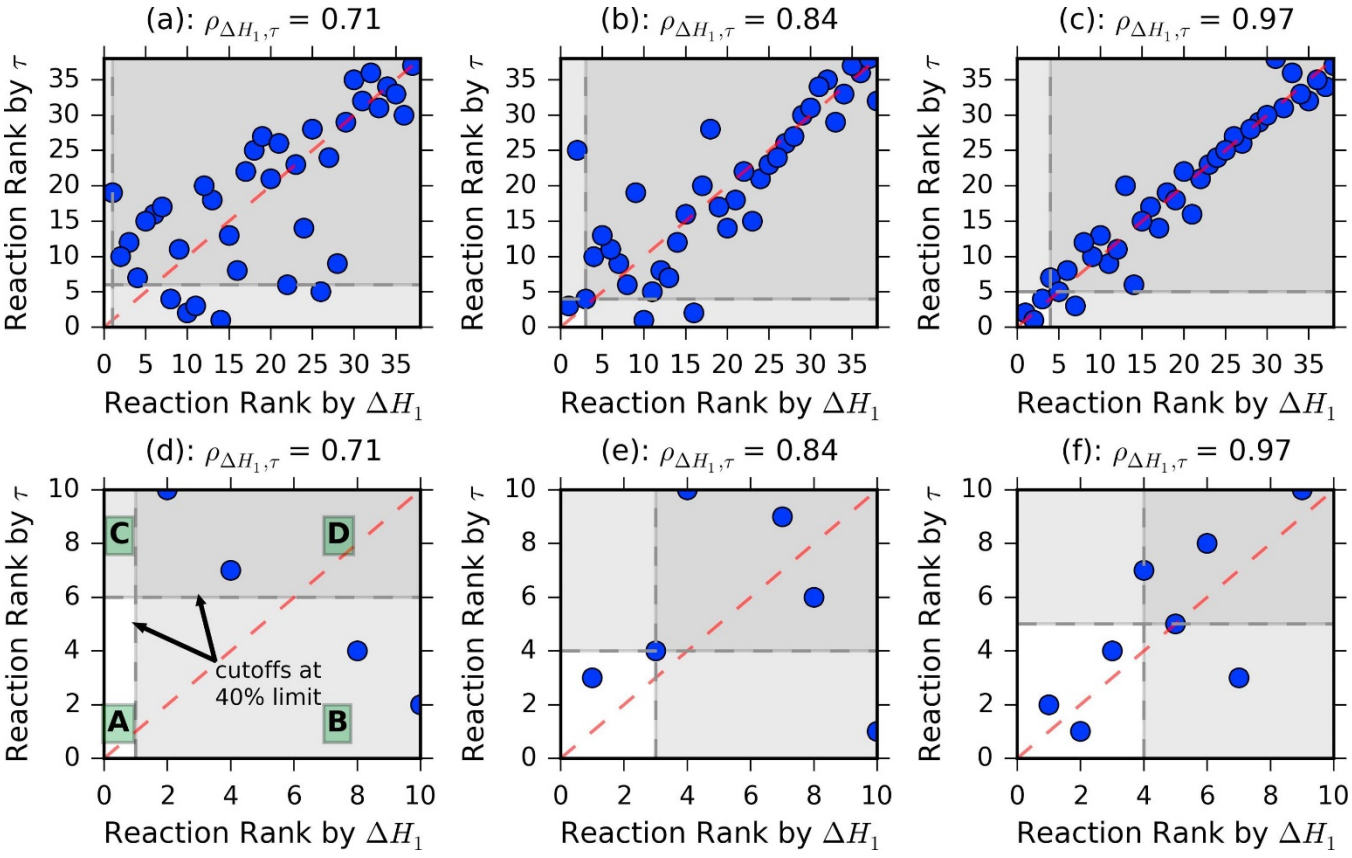

Fig. 3. Comparison of reaction rankings by ΔH_1 and by τ for rank correlation coefficients of $\rho_{\Delta H_1,\tau} = 0.71$ (a and d), $\rho_{\Delta H_1,\tau} = 0.84$ (b and e), and $\rho_{\Delta H_1,\tau} = 0.97$ (c and f). The plots in (a), (b), and (c) are scaled to show the full ranking comparison, and the same data is shown in plots (d), (e), and (f), respectively, but with a reduced scale. The dashed lines represent the lowest ranking reaction that has a percent sensitivity of at least 40% of the maximum percent sensitivity observed at a given condition. These cutoff lines can be used to divide the plane into four regions, (A), (B), (C), and (D).

Table 2 summarizes the average number of reactions that fall within each of the regions (A), (B), (C), and (D) for varying intervals of $\rho_{\Delta H_1,\tau}$ As expected, the highest bin count for region (A) corresponds to the highest interval for the rank correlation coefficient, $0.9 \leq \rho_{\Delta H_1,\tau} \leq 1.0$. However, even when the agreement in the rankings is characterized by $\rho_{\Delta H_1,\tau}$ values in excess of 0.9, there are still reactions that fall within regions (B) and (C), again suggesting that the metrics of ΔH_1 and τ are complementary. As $\rho_{\Delta H_1,\tau}$ decreases, the number of reactions in region (A) decreases and then goes to zero. The number of reactions in region (D) remains relatively constant during this decrease in $\rho_{\Delta H_1,\tau}$, which implies reactions are redistributed from region (A) into regions (B) and (C), with a preponderance of the reactions going to region (B). The average number of reactions that are binned in region (C) varies between limits of only 1.2 and 3.0, and does not exhibit strong sensitivity to decreasing $\rho_{\Delta H_1,\tau}$. From a practical standpoint, this indicates that the decreasing value $\rho_{\Delta H_1,\tau}$ is primarily driven by low-rank reactions, and that the number of influential, high-rank reactions that are not accounted for by S_τ may reach an upper limit.

Table 2. Average bin counts for regions A, B, C, and D for varying $\rho_{\Delta H_1,\tau}$ intervals.

	Region			
	A	**B**	**C**	**D**
$0.9 \le \rho_{\Delta H_1,\tau} \le 1.0$	3.5	2.8	1.2	30.4
$0.8 \le \rho_{\Delta H_1,\tau} < 0.9$	1.6	3.8	2.1	30.5
$0.7 \le \rho_{\Delta H_1,\tau} < 0.8$	0.6	5.3	3.0	29.2
$0.6 \le \rho_{\Delta H_1,\tau} < 0.7$	0.0	6.2	2.4	29.4
Averages	1.4	4.5	2.2	29.9

3.3. Comparison of high-rank reactions

This section compares the agreement between rankings for the three most influential reactions, as determined using the four metrics of ΔH_1, τ, τ_1, and ΔP_1. Special attention is given to the top three reactions because they represent a reasonable upper limit for the number of reactions that may be considered for improvement in a study. The results appear in Table 3, which lists all reactions that existed in the top-three ranking at least once during the analysis. The table is organized to show the frequency with which each reaction was ranked in position (1), (2), or (3) according to each of the metrics.

Table 3. Summary of agreement between sensitivity analyses based unique metrics.

Reactions	ΔH_1 **Rank Frequencies**			τ **Rank Frequencies**			τ_1 **Rank Frequencies**			ΔP_1 **Rank Frequencies**		
	(1)	**(2)**	**(3)**	**(1)**	**(2)**	**(3)**	**(1)**	**(2)**	**(3)**	**(1)**	**(2)**	**(3)**
(R1) $C_7H_{16} + O_2 \Leftrightarrow C_7H_{15} + HO_2$	1	2	1									
(R3) $C_7H_{15}O_2 \Leftrightarrow C_7H_{14}OOH$	29	7	14	7	34	27		234	30	22	29	23
(R4) $C_7H_{14}OOH + O_2 \Leftrightarrow O_2C_7H_{14}OOH$	2	2				1			148		3	7
(R6) $C_7KET \Rightarrow C_5H_{11}CO + CH_2O + OH$	3	5	7	37	21	38	280			27	37	34
(R8) $C_7H_{16} + OH \Rightarrow C_7H_{15} + H_2O$	130	61	26						16	52	48	21
(R9) $C_7H_{15} + O_2 \Leftrightarrow C_7H_{14} + HO_2$	3	6	3			1			19	9	2	
(R11) $C_7H_{16} + HO_2 \Leftrightarrow C_7H_{15} + H_2O_2$			1									
(R15) $C_8H_{17} + O_2 \Leftrightarrow C_8H_{17}O_2$	1	27	38								3	43
(R16) $C_8H_{17}O_2 \Leftrightarrow C_8H_{16}OOH$			2									
(R17) $C_8H_{16}OOH + O_2 \Leftrightarrow O_2C_8H_{16}OOH$			3									1
(R21) $C_8H_{18} + OH \Rightarrow C_8H_{17} + H_2O$	96	61	34		23	78		46	67	161	26	16
(R22) $C_8H_{17} + O_2 \Leftrightarrow C_8H_{16} + HO_2$	1	1	6									21
(R29) $C_2H_4 + OH \Leftrightarrow C_2H_3 + H_2O$			8									
(R31) $CH_2O + OH \Leftrightarrow HCO + H_2O$	8	88	30	36	18	21				9	109	28
(R34) $H_2O_2 + OH \Leftrightarrow HO_2 + H_2O$	4	20	107			34					23	84
(R37) $H_2O_2 + M \Leftrightarrow OH + OH + M$				2	158	44						
(R38) $C_2H_4 + O_2 \Rightarrow CH_2O + CH_2O$	2			198	26	36						2

The results reveal that the ΔH_1 metric is influenced by a broader array of reactions (16 reactions) than the metrics of τ or τ_1 (9 and 6 reactions, respectively). This suggests that the overall shape of the heat

release curve exhibits greater sensitivity to more of the kinetic model than the metrics of τ or τ_1. The two most influential reactions for ΔH_1 are the hydrogen abstraction reactions from the fuel molecules by OH (reactions R8 and R21), and neither of these ever appear as the most influential reaction for τ or τ_1. The hydrogen abstraction reaction from iso-octane (R21) is ranked in positions (2) and (3) according to τ under some conditions, but the hydrogen abstraction reaction from *n*-heptane (R8) never appears in the top three ranking. It is important to note that for 198 of the 280 simulations, the most important reaction for τ was the global reaction of $C_2H_4 + O_2 \Rightarrow CH_2O + CH_2O$ (R38). This reaction was included in the Tsurushima mechanism to improve the agreement of CH_2O predictions with HCCI engine data [12], and it dominates the global ignition response for many of the simulated conditions. Despite its overwhelming influence, the roles of the elementary reactions in the remaining rankings are still substantially different for τ than for ΔH_1. The discrepancies in the sets of important elementary reactions also imply that similar results may be obtained if a detailed mechanism had been used. It is well known that only a small fraction of the reactions within a detailed mechanism are important for producing global ignition behavior. This reaction set must constitute the important reaction classes for two-stage ignition behavior that appear in Table 3. If the sensitivity analysis had been done with a full detailed mechanism, these important reaction classes would be retained and their influence would be made evident with respect to the individual features of autoignition that they influence (*i.e.*, τ_1, ΔH_1, etc.)

The histogram results in Fig. 2(b) implied markedly different global reaction rankings according to ΔH_1 and τ_1, and Table 3 shows that the rankings have only mild resemblance when considering just the three most influential reactions. According to S_{τ_1}, the most influential reaction for all simulations was the unimolecular decomposition of the C7-ketohydroperoxide (R6). The rate constants for this reaction were obtained from the ketohydroperoxide decomposition reaction of Tanaka et al. [13], ($C_7KET \Rightarrow OC_7H_{13}O + OH$), however, the reaction products were modified to include CH_2O to moderate the energy release rate during fuel consumption. Isomerization of the heptylperoxy radical ($C_7H_{15}O_2$) according to reaction R3 was also influential for τ_1, ranking as the second most important reaction for 234 of the 280 simulations. Table 3 shows this same reaction is also influential for ΔH_1 under some conditions. The greatest similarity between the $S_{\Delta H_1}$ -based and S_{τ_1} -based rankings occurs for the H-abstraction reaction of $C_8H_{18} + OH \Rightarrow C_8H_{17} + H_2O$ (R21).

The rankings according to $S_{\Delta P_1}$ are also shown in Table 3 because ΔH_1 cannot be measured in a RCM experiment. Overall, there is a strong resemblance between the list of reactions that are influential to these metrics, but some important discrepancies exist, indicating there is value in studying both ΔP_1 and ΔH_1. The ΔP_1 rank frequencies show a substantial shift away from reaction R8, with only 52 cases identifying this reaction as the most important reaction, as compared to being the most important reaction in 130 of the cases according to $S_{\Delta H_1}$ In 48 of those 130 cases, the most important reaction became R21 ($C_8H_{18} + OH \Rightarrow C_8H_{17} + H_2O$) when ranking by $S_{\Delta P_1}$ instead of $S_{\Delta H_1}$. This shift accounts for most of the increase in rank frequency for reaction R21 that is observed in Table 3, where it is the most important reaction in 161 of 280 of the cases. Relative to ΔH_1, the ΔP_1 rank frequencies also more frequently list reaction R6 as influential. The discrepancy between the $S_{\Delta H_1}$ -based and $S_{\Delta P_1}$ -based rankings arises due to the coupled physical and chemical effects that are present in the ΔP_1 characterization. In addition to the energy release, pressure in the RCM cylinder is affected by compression, heat loss, and crevice flow. Significant chemical energy release during rapid transients that are associated with these physical processes may be overwhelmed, thus masking the roles of individual reactions. As described above, heat release rate and therefore ΔH_1 cannot be measured in the RCM, however, it is possible to develop a model to estimate ΔH_1 from experimental data.

3.4. Influence of reaction conditions on rank agreement

The results in Sections 3.1 Overall comparison of rankings, 3.2 Illustration, significance, and trends of the rankings, 3.3 Comparison of high-rank reactions demonstrate that the agreement between the reaction rankings based on $S_{\Delta H_1}$ and S_τ can vary substantially. The analysis in this section is intended to determine which reaction conditions lead to good or poor agreement as characterized by Spearman's rank correlation coefficient. The results of this analysis appear in Fig. 4, where scatterplots are presented according to different combinations of the following reaction parameters: *ON*, ϕ, T_c, and P_c. The color of each point in the scatterplot corresponds to the rank correlation coefficient, $\rho_{\Delta H_1,\tau}$, and the authors emphasize that the rankings are performed within each individual test condition. The overall "shape" of the scatterplots is determined by the selection procedure described in Section 2.3, as selected points were targeted to have a minimum $\tau_1 \sim 10$ ms and maximum $\tau \sim 150$ ms. The first three scatterplots, in Fig. 4(a)–(c) clearly show that the *ON* is very influential for determining the rank correlation coefficient, where it appears that $\rho_{\Delta H_1,\tau}$ is directly proportional to *ON*. This may imply that long ignition delay times associated with increasing amounts of iso-octane lead to greater agreement between the reaction sensitivities for ΔH_1 and τ. Further analysis on this topic appears in Section 3.5. Another, more mild trend, can be seen in Fig. 4(a) and (b), where it appears that $\rho_{\Delta H_1,\tau}$ may be inversely proportional to both ϕ, and T_c. This relationship appears in the region where *ON* < 20, and it implies that greater reactivity, as characterized by higher temperatures and equivalence ratios, leads to less agreement between $S_{\Delta H_1}$ -based and S_τ -based rankings. However, Fig. 4(d) indicates that this interpretation is not valid for all cases because the points of both high and low rank correlation coefficients are located in the region of high T_c and high ϕ. It should be noted that negative temperature coefficient behavior (NTC) is not predicted by the Tsurushima mechanism for temperatures less than 750 K, meaning these results are not influenced by a phenomenological shift in ignition behavior between the low-temperature and NTC regions. The remaining plots in Fig. 4(c), (e), and (f) do not display any strong trends that are not captured by the other plots.

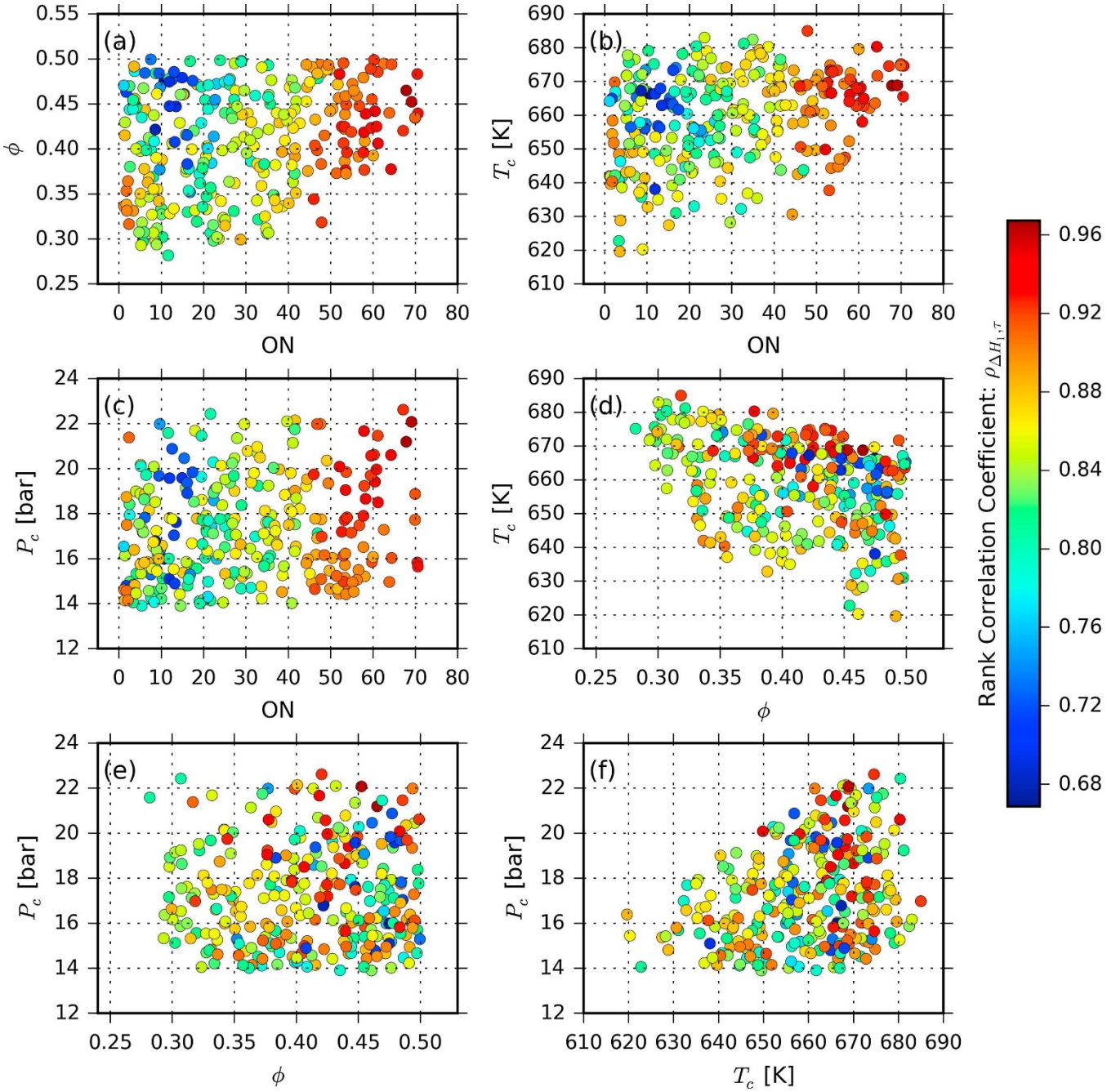

Fig. 4. Scatterplots showing rank correlation coefficient, $\rho_{\Delta H_1,\tau}$, as a function of the simulation reaction conditions. The markers are colored according to the value of $\rho_{\Delta H_1,\tau}$ calculated using the sensitivity analysis at each simulation condition.

3.5. Influence of reaction behavior on rank agreement

The analysis in the previous section demonstrated that the rank correlation coefficient, $\rho_{\Delta H_1,\tau}$, is dependent on the reaction conditions. Further analysis is conducted here to characterize the reaction behavior or phenomenology that leads to this dependence. Fig. 5 shows scatterplots of the simulation results that are organized by *ON* (abscissa in all cases) with the points shaded according to $\rho_{\Delta H_1,\tau}$. The following ignition metrics are used as the ordinates in the subplots: (a) τ_1, (b) τ, (c) ΔH_1 and (d) HRR_{max}. HRR_{max} is the maximum heat release rate observed during the first stage of ignition. *ON* is

used as the abscissa in all of the plots because the analysis of Fig. 4 demonstrated that it strongly influences $\rho_{\Delta H_1,\tau}$. The direct proportionality of $\rho_{\Delta H_1,\tau}$ to *ON* is evident in all of the subplots in Fig. 5.

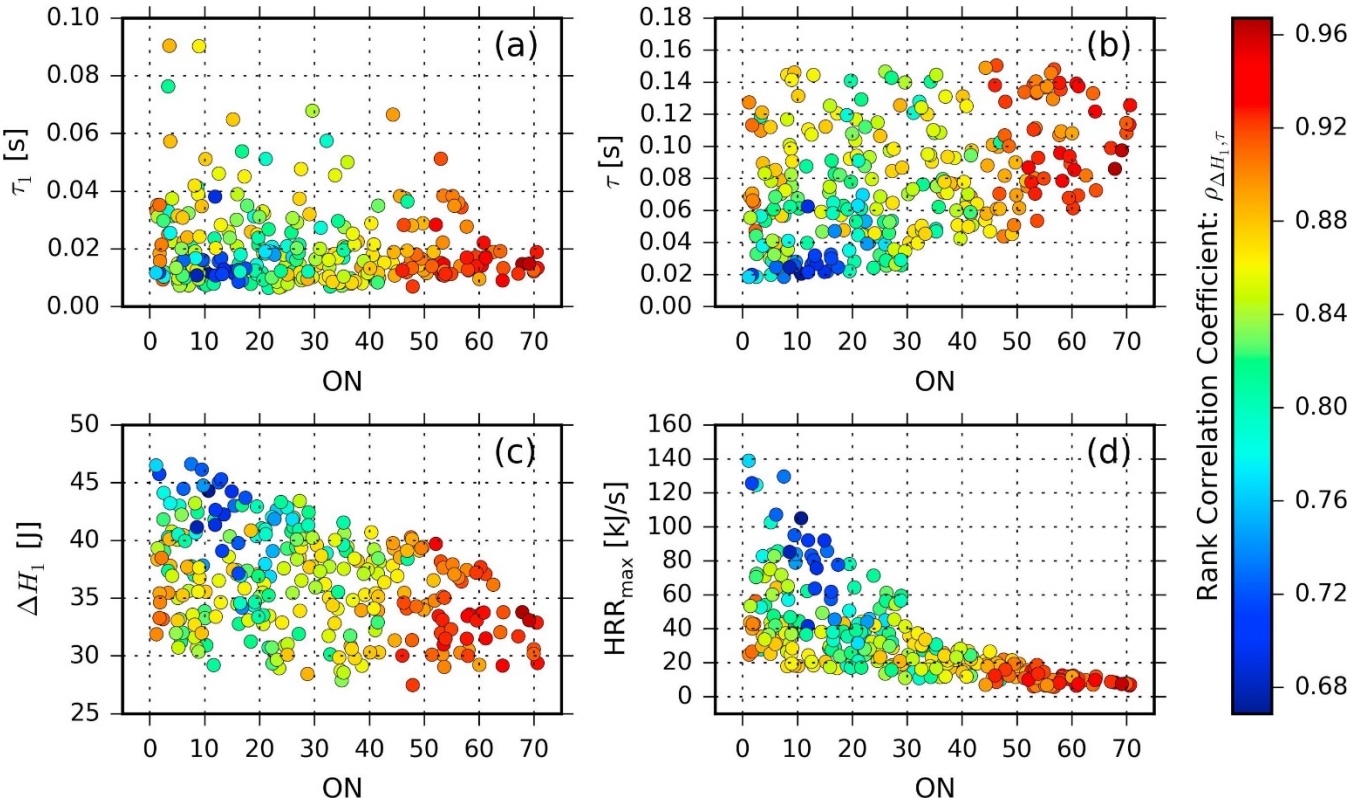

Fig. 5. Rank correlation coefficient ($\rho_{\Delta H_1,\tau}$) as a function of *ON* and ignition metrics: (a) τ_1, (b) τ, (c) ΔH_1, and (d) HRR_{max}. Each marker is colored according to the value of $\rho_{\Delta H_1,\tau}$ calculated from the sensitivity runs.

Fig. 5(a) and (b) show that the simulations with the lowest rank correlation coefficient are clustered around short ignition delay times. Close inspection of the data in Fig. 5(b) shows that the shortest total ignition delay times (τ) all have low rank correlation coefficients. By necessity, these simulations also have short first stage ignition delay times (*i.e.*, τ_1 must be less than τ), however, the data in Fig. 5(a) show that it is possible to have a short τ_1 and a modest rank correlation coefficient ($0.80 \leq \rho_{\Delta H_1,\tau} \leq 0.86$). The highest rank correlation coefficients are shifted toward higher *ON* and longer ignition delay times, meaning $S_{\Delta H_1}$-based and S_τ-based reaction rankings are similar for high octane number tests, and that little new kinetic information may be obtained by studying ΔH_1 in addition to τ. By contrast, low octane number tests have more variability among these two sets of reaction rankings, allowing for additional kinetic information to be obtained by characterizing ΔH_1 and its sensitivities. Support for the interpretation that the value of ΔH_1 as a diagnostic depends on *ON* is also present in Table 3. For higher ON fuels, reaction R21 becomes increasingly important ($C_8H_{18} + OH \Rightarrow C_8H_{17} + H_2O$). This reaction was ranked within the top three by both $S_{\Delta H_1}$ and S_τ for multiple cases. However, the analogous H-abstraction reaction for *n*—heptane (reaction R8, $C_7H_{16} + OH \Rightarrow C_7H_{15} + H_2O$), which would be increasingly important for low ON fuels, is only ranked within the top three by $S_{\Delta H_1}$. It is never ranked within the top three by the S_τ sensitivity coefficient.

The data in Fig. 5(c) and (d) are important for explaining the different heat release characteristics that influence $\rho_{\Delta H_1,\tau}$. The data in Fig. 5(c) clearly show that as the first stage heat release increases (ΔH_1), a greater disparity may exist between the $S_{\Delta H_1}$-based and S_τ-based rankings. This is primarily evident

for the *ON* < 20 region. The higher *ON* simulations do not appear to be influenced by this trend, thus we suspect an additional reaction parameter is important. The data in Fig. 5(d) suggest that this parameter is the maximum heat release rate (HRR_{max}). The data show that for *ON* > 40, the HRR_{max} values are small and the $\rho_{\Delta H_1,\tau}$ values are high (many cases $\rho_{\Delta H_1,\tau}$ > 0.92). However, for decreasing *ON* and large HRR_{max}, the rank correlation coefficient is diminished. It is evident that $\rho_{\Delta H_1,\tau}$ is minimized for low *ON* simulations that possess the highest HRR_{max} values. Many of the low *ON* simulations with HRR_{max} < 60 kJ/s have modest rank correlation coefficients in the approximate range of 0.80 ≤ $\rho_{\Delta H_1,\tau}$ ≤ 0.89. These simulations, with their lower HRR_{max} values, correspond to cases with low ϕ and/or low T_c, and the results support the overall interpretation that $\rho_{\Delta H_1,\tau}$ is a function of *ON*, ϕ, and T_c. For combinations of these three parameters that lead to rapid heat release rate (i.e., large HRR_{max}), the rank correlation coefficient ($\rho_{\Delta H_1,\tau}$) is minimized and distinct kinetic information can be obtained by studying ΔH_1 and τ.

3.6. Explanation of reaction phenomenology

The results and analysis in Sections 3.4 Influence of reaction conditions on rank agreement, 3.5 Influence of reaction behavior on rank agreement characterize the reaction conditions and behavior that lead to low $\rho_{\Delta H_1,\tau}$ values, but they do not describe the physical reason for these low $\rho_{\Delta H_1,\tau}$ values. In other words, why do large values of HRR_{max} lead to disagreement between $S_{\Delta H_1}$ -based and S_τ -based rankings? It was hypothesized that a low rank correlation coefficient results when the most reactive zone determines τ and a broad distribution of zones (*i.e.*, reaction conditions) determine ΔH_1. To test this hypothesis, additional simulations were conducted to calculate the total energy released during the first stage of ignition in each of the zones. The results were used to calculate the energy release for a range of temperatures, as shown in Fig. 6. Three cases of varying $\rho_{\Delta H_1,\tau}$ are considered in the figure, and they show that as $\rho_{\Delta H_1,\tau}$ decreases, an increasingly broad distribution of temperatures contributes to the first stage energy release. The temperature spans contributing at least 1% of the total cylinder first stage energy release are 83 K, 105 K, and 135 K for the $\rho_{\Delta H_1,\tau} = 0.97$, $\rho_{\Delta H_1,\tau} = 0.85$, and $\rho_{\Delta H_1,\tau} = 0.70$ cases, respectively. A broad range of reaction conditions that contribute to energy release provides a mechanism for a larger set of reactions to play an influential role in ΔH_1. By contrast, the onset of ignition is determined by the hottest conditions in the simulations, and it is noted that the fraction of first stage energy release that occurs in the highest temperature bin decreases as $\rho_{\Delta H_1,\tau}$ decreases. Specifically, for the three cases of $\rho_{\Delta H_1,\tau} = 0.97$, $\rho_{\Delta H_1,\tau} = 0.85$, and $\rho_{\Delta H_1,\tau} = 0.70$, the highest temperature bin contributes 9%, 7% and 6% of the total first stage energy release, respectively.

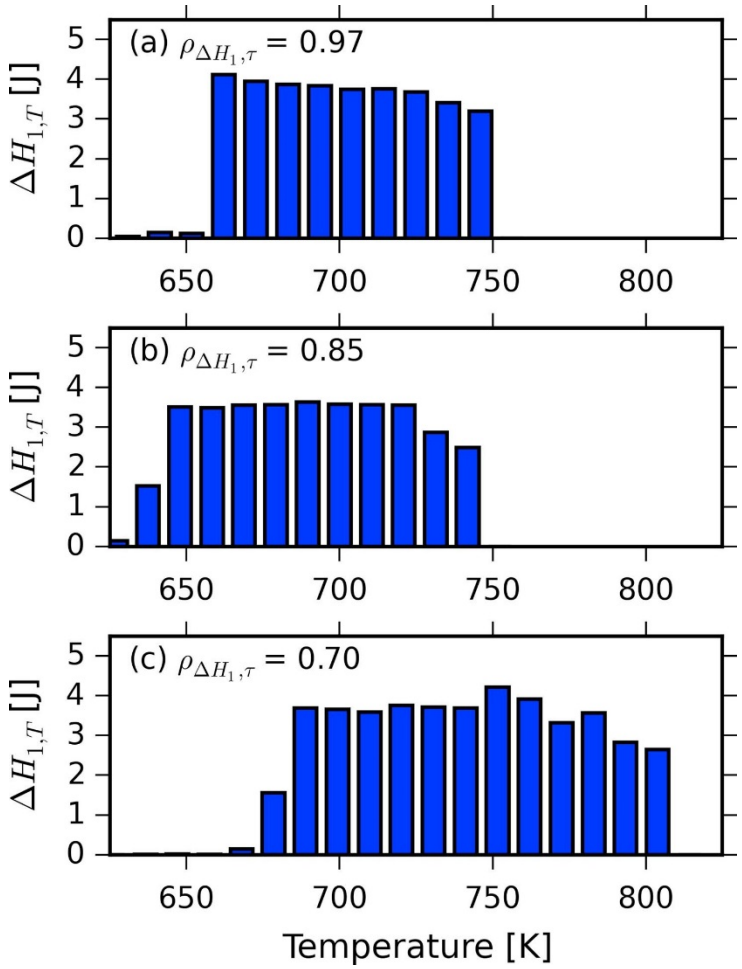

Fig. 6. Histograms showing total heat release during the first stage of ignition according to the temperature at which the energy is being released. The temperature bins have a width of 10 K. Results appear for three cases: (a) $\rho_{\Delta H_1,\tau} = 0.97$, (b) $\rho_{\Delta H_1,\tau} = 0.85$, and (c) $\rho_{\Delta H_1,\tau} = 0.70$.

4. Conclusion

This study used a simulation-based method for investigating the reaction sensitivities of the ignition metrics ΔH_1, ΔP_1, τ, and τ_1 during two-stage ignition in a RCM. The simulations targeted the low-temperature, lean conditions relevant to advanced engines, and utilized a multi-zone RCM model coupled with a skeletal PRF mechanism. The goal of the study was to determine whether new kinetic information could be obtained by studying the metrics ΔH_1 and ΔP_1 in addition to τ and τ_1. The following conclusions are drawn from the results:

- Significant disagreement exists between the reaction rankings based on ΔH_1 and τ_1. This discrepancy was used to justify more rigorous study of the ΔH_1 -τ relationship.
- The agreement between $S_{\Delta H_1}$ -based and S_τ -based rankings varies substantially depending on reaction conditions. Increasingly reactive conditions, as characterized by low octane number, high T_c and high ϕ, lead to poor agreement between the two sets of rankings. Under these conditions ($\rho_{\Delta H_1,\tau}$), new kinetic information can be obtained by studying ΔH_1. These results may be especially important for characterizing experiments conducted at stoichiometric or rich conditions, where greater reactivity is observed. Estimation of ΔH_1 can be made especially useful with the simultaneous measurement of RCM gas temperature [15].

- Poor agreement between the $S_{\Delta H_1}$ -based and S_τ -based rankings occurs because of the distribution of reaction conditions that develop in the highly reactive cases. Energy release occurs in these cases across a temperature range in excess of 100 K. This broad distribution provides a pathway for additional reactions to influence the first stage energy release, leading to a set of sensitivity coefficients that are unique from those obtained by studying τ and τ_1.
- Despite the practicality of measuring ΔP_1, it is an inferior validation metric relative to ΔH_1. A model-based approach should be considered to estimate ΔH_1 from experimental data, but its value as a validation metric will be highly dependent on the rigor of the estimation model.

Acknowledgements

Acknowledgement is made to the Donors of the American Chemical Society Petroleum Research Fund 53521-DNI6 for support of this research.

References

[1]S. Tanaka, F. Ayala, J.C. Keck, J.B. Heywood. Two-stage ignition in HCCI combustion and HCCI control by fuels and additives. *Combust Flame*, 132 (1–2) (2003), pp. 219-239.

[2]M. Ribaucour, R. Minetti, L.R. Sochet, H.J. Curran, W.J. Pitz, C.K. Westbrook. Ignition of isomers of pentane: an experimental and kinetic modeling study. *Proc Combust Inst*, 28 (2) (2000), pp. 1671-1678.

[3]C.K. Westbrook. Chemical kinetics of hydrocarbon ignition in practical combustion systems. *Proc Combust Inst,* 28 (2) (Jan. 2000), pp. 1563-1577.

[4]P. Zhang, W. Ji, T. He, X. He, Z. Wang, B. Yang, *et al.* First-stage ignition delay in the negative temperature coefficient behavior: experiment and simulation. *Combust Flame*, 167 (2016), pp. 14-23.

[5]P. Zhao, C.K. Law. The role of global and detailed kinetics in the first-stage ignition delay in NTC-affected phenomena. *Combust Flame*, 160 (11) (2013), pp. 2352-2358.

[6]G. Mittal, M. Chaos, C.-J. Sung, F.L. Dryer. Dimethyl ether autoignition in a rapid compression machine: experiments and chemical kinetic modeling. *Fuel Process Technol*, 89 (12) (Dec. 2008), pp. 1244-1254.

[7]G. Kukkadapu, K. Kumar, C.-J. Sung, M. Mehl, W.J. Pitz. Autoignition of gasoline surrogates at low temperature combustion conditions. *Combust Flame*, 162 (5) (2015), pp. 2272-2285.

[8]G. Kukkadapu, K. Kumar, C.-J. Sung, M. Mehl, W.J. Pitz. Experimental and surrogate modeling study of gasoline ignition in a rapid compression machine. *Combust Flame*, 159 (10) (Oct. 2012), pp. 3066-3078.

[9]D. Wilson, C. Allen. Application of a multi-zone model for the prediction of species concentrations in rapid compression machine experiments. *Combust Flame*, 171 (2016), pp. 185-197.

[10]S.S. Goldsborough, C. Banyon, G. Mittal. A computationally efficient, physics-based model for simulating heat loss during compression and the delay period in RCM experiments**.** *Combust Flame*, 159 (12) (Dec. 2012), pp. 3476-3492.

[11]S.S. Goldsborough, G. Mittal, C. Banyon. Methodology to account for multi-stage ignition phenomena during simulations of RCM experiments. *Proc Combust Inst*, 34 (Jul. 2013), pp. 685-693.

[12]T. Tsurushima. A new skeletal PRF kinetic model for HCCI combustion. *Proc Combust Inst*, vol. 32 II (2) (2009), pp. 2835-2841.

[13]S. Tanaka, F. Ayala, J.C. Keck. A reduced chemical kinetic model for HCCI combustion of primary reference fuels in a rapid compression machine. *Combust Flame*, 133 (4) (Jun. 2003), pp. 467-481.

[14]C. Spearman. The proof and measurement of association between two things. *Am J Psychol*, 15 (1) (1904), pp. 72-101.
[15]E.F. Nasir, A. Farooq. Time-resolved temperature measurements in a rapid compression machine using quantum cascade laser absorption in the intrapulse mode. Proc Combust Inst, 36 (3) (2017), pp. 4453-4460.